Immobilization of Silanized DNA on Glass: Influence of the Silane Tether on the DNA Hybridization

T. Solomun,*,† R. Mix,† and H. Sturm*,†,§

Institute of Chemistry and Biochemistry, Free University Berlin, Takustrasse 3, D-14195 Berlin, Germany, Federal Institute for Materials Research and Testing, Unter den Eichen 87, D-12205 Berlin, Germany, Institute of Machine Tools and Factory Management, Technical University of Berlin, Pascalstrasse 8-9, D-10587 Berlin, Germany

ABSTRACT Two trifunctional (trimethoxy and triethoxy) and one difunctional (methyldimethoxy) 3-mercaptopropyl-alkoxysilanes were covalently tethered to thiolated DNA oligonucleotides in solution. After deposition as microarrays onto glass, the immobilized DNA probes were tested for hybridization ability by a florescence-based method. The results demonstrate a large enhancement in the fluorescence signal when the functionality of the silane tether is reduced from three to two. An XPS analyses revealed that this is not due to a higher DNA surface density. FTIR spectra of the spin-coated silanes showed that the trifunctional silanes form branched and cyclic siloxane moieties, whereas the difunctional silane generates predominantly short straight siloxane chains. Therefore, the propensity of trifunctional silanes to form more complex networks leads to conformations of the bound DNA which are less favorable for the specific interaction with the complementary strand. The data implicate that further significant improvements in the DNA hybridization ability are possible by adroit choice of the silane system.

KEYWORDS: silanized DNA • DNA immobilization • DNA hybridization • fluorescence imaging • FTIRS • XPS.

INTRODUCTION

Immobilization of DNA molecules onto a solid surface that permits their accessibility for binding with the complementary strands is a decisive first step to implement a variety of important technologies such as gene expression (1), biomolecular computation (2), advanced molecular devices (3), and biosensors (4). Therefore, numerous studies have been devoted to immobilizing DNA molecules on solid surfaces (5−8). Glass slides are still generally favored for the DNA microarray applications. The central question here is the development of efficient chemistries for covalent attachment of DNA. A great number of attachment methods have been published, which vary widely in chemical mechanisms, ease of use, probe density and stability (9−12). Most of these procedures are laborious and time-consuming because they involve modifications of glass or silicon surfaces in order to achieve reactivity against corresponding (modified) DNA. For this reasons, the development of direct deposition methods, such as the one based on coupling of silanized DNA to unmodified glass surface (13), is technologically important. The above method involves covalent conjugation of an active silyl moiety to DNA in a solution and simultaneous deposition onto glass (13). An important advantage here is low background fluorescence compared with modified surfaces such as composed of polylysine or aminosilane coating. However, a recent study (14) raised a question of low accessibility of the deposited silanized DNA despite its apparently high surface coverage. On the other hand, it is know from previous work (15, 16) that the interaction of alkoxysilanes with SiO_2 type of surfaces strongly depends on the number of the active alkoxy groups. This should also influence the properties of silanized DNA immobilized on glass. Here we report on the impact of the functionality of 3-mercaptopropyl silanes tethers on the surface DNA hybridization ability.

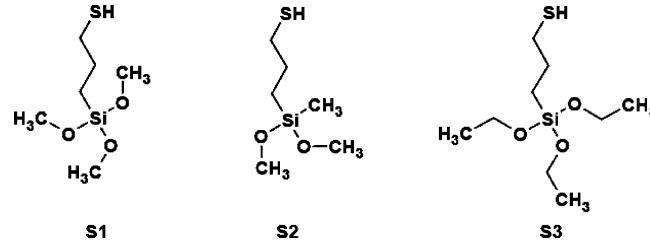

FIGURE 1. Chemical structures of the silanes used in this study: (3-mercaptopropyl)trimethoxysilane (S1), (3-mercaptopropyl)methyldimethoxysilane (S2), (3-mercaptopropyl)triethoxysilane (S3).

EXPERIMENTAL SECTION

The chemical structures of the three mercaptopropyl-silanes (Aldrich, > 95%) are shown in Figure 1. Silanes S1 and S3 have three active methoxy and ethoxy groups, respectively. Silane S2 has an inactive methyl group, in addition to two methoxy groups. Corresponding monofunctional mercaptosilanes are not commercially available.

The single-stranded DNA oligonucleotides were obtained from Thermo Electron (Germany). They were purified by HPLC and had the following structures:

* Corresponding author. E-mail: solomun@chemie.fu-berlin.de. (T.S.); heinz.sturm@bam.de. (H.S.).
Received for review March 25, 2010 and accepted July 14, 2010
† Free University Berlin.
‡ Federal Institute for Materials Research and Testing.
§ Technical University of Berlin.
DOI: 10.1021/am100263t

O1 = 5′-ACG ACG GCC AGT GAA TTC GAG CTC GGT ACC

O1-SH = 5′- HS-$(CH_2)_5$-ACG ACG GCC AGT GAA TTC GAG CTC GGT ACC

O1Rev-SH = 5′- HS-$(CH_2)_5$-CCA TGG CTC GAG CTT AAG TGA CCG GCA GCA

Comp-O1 = 5′-Cy5-GGT ACC GAG CTC GAA TTC AC.

The Cy5-dye labeled oligonucleotide Comp-O1 is complementary to the 20-mer sequence of the O1 and O1-SH oligonucleotides at its 3′-end, but it is not complementary to the O1Rev-SH oligonucleotide, which has the reverse O1 sequence. Glass slides (Menzel, Germany) and gold chips (Arrandee, Germany) were cleaned by a brief dipping into hot nitric acid, followed by washing with copious amounts of ultra pure water (Merck, HPLC grade) and drying with nitrogen. Silane solutions were prepared as the 1 mM stock solutions in NaOAc (sodium acetate) buffer (30 mM, pH 4.3). The oligonucleotides were dissolved in the same buffer to the 200 μM stock solutions, divided into aliquots and stored until use at −20 °C. From the two stock solutions, 20 μL of the mixed solution was prepared with a DNA:silane concentration of 1:5 (50 μM DNA and 250 μM silane). The solutions were allowed to react for 2 h before the deposition onto glass. Thereby, covalent disulfide bonds between the thiol ends of DNA and silane are formed, resulting in silanized DNA.

Microarray Fluorescence Measurements. Ten microliters of the solution for each silane system were transferred to a microtiterplate and deposited as microarrays on six glass slides using a Genetix QArray Microarrayer and Telechem (Sunnyvale, CA, USA) SMP4 split pin producing the spots of about 120 μm in diameter. For each oligonucleotide (O1, O1-SH, and O1Rev-SH) two different sets of microarrays (10 × 6 and 4 × 4) were printed 2-fold on each slide. After the printing the slides were left for 30 min in humid atmosphere (70%) and then dipped for 30s into boiling water to remove noncovalently bound DNA (13), following by drying with nitrogen. The hybridization with the dye-labeled Comp-O1 oligonucleotide was carried-out overnight (5 μM Comp-O1 in 3xSSC). Following this, the slides were washed three times with 3 × SSC + 0.1% Tweed (3 min under shaking), two times with 1 × SSC + 0.1% Tweed (15 min under shaking), and further washed with copious amounts of ultra pure water and finally dried with nitrogen. The slides were scanned using an Affymetrix 418 Array Scanner. The fluorescence microarray images were analyzed with the GenePixPro6 software with the local background subtraction at the diameter three times of the spot size.

XPS Measurements. The X-ray spectra were obtained using a SAGE 150 Spectrometer (Specs, Germany), a Al−Kα radiation source, an energy analyzer pass energy of 20 eV and 90° takeoff angle geometry. For the XPS measurements, 12 mm diameter glass coverslips (Menzel, Germany) were immersed completely in the corresponding silane-DNA solutions for 2 h, following by washing and 30s immersion into boiling water.

FTIRS Measurements. Infrared data were obtained with a FTIR spectrometer (Nicolet 6700) purged with nitrogen and equipped with the external reflection accessory (85° grazing angle) and a MCT detector. Thin-films of the silanes were deposited onto gold-on-glass chips by spin-coating (60s at 3000 rpm, 10 mM silane in NaOAc buffer, pH 4.3) and immediately transferred into the FTIR spectrometer for the reflection−absorption measurements.

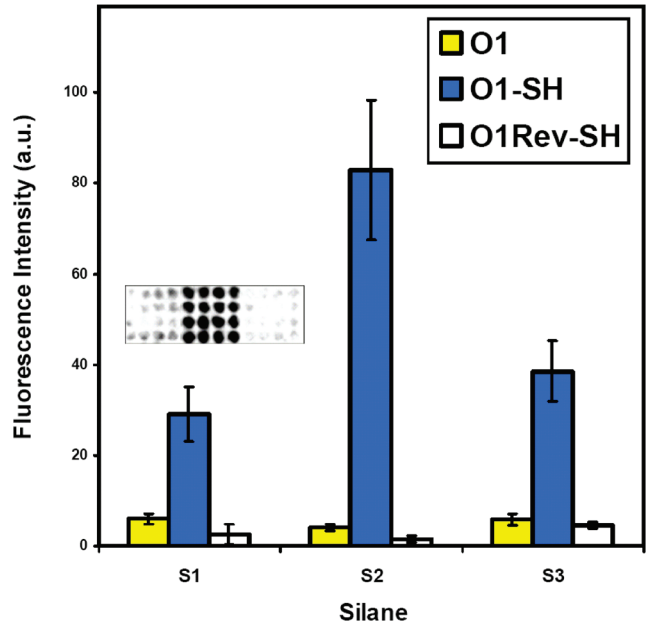

FIGURE 2. Dependence of the hybridization reaction on the silane structure. For each silane the data using either (a) nonthiolated, cDNA (O1, left column);, (b) thiolated and cDNA sequence (O1-SH, center column); or (c) thiolated, but noncDNA (O1Rev-SH, right column) are presented. Inset: Example of the 4 × 4 microarrays for S1 and the cases a−c (from left to right). S1, (3-mercaptopropyl)-trimethoxysilane; S2, (3-mercaptopropyl)-methyldimethoxysilane; S3, (3-mercaptopropyl)-triethoxysilane.

RESULTS AND DISCUSSION

Figure 2 shows the data on the DNA hybridization as a function of the type of the silane tether. The hybridization is probed by the fluorescence intensity of the Cy5-dye on the complementary strand. In Figure 2 the data are presented for the cases when: (a) the DNA is complementary to the dye-labeled strand but does not contain the thiolated end, and, therefore, does not covalently bind silane, (b) the DNA is thiolated and complementary, and (c) the DNA is thiolated, but noncomplementary to the dye-labeled strand. Cases a and c are negative control cases. The very low intensities of the corresponding microarrays for all three silanes, as compared to the case of the complementary and thiolated DNA (case b), demonstrate the high selectivity of the method. For the systems using the complementary and thiolated DNA, the important result is the systematically observed much higher fluorescence intensity (by about a factor of 2−3) in the case of the difunctional silane S2, as compared to the trifunctional silanes S1 or S3.

To determine if this is due to a higher surface coverage of DNA in the case of the bifunctional silane or due to other effects, such as silane induced DNA conformations which are nonfavorable for the hybridization reaction, we have carried-out XPS measurements on glass coated with si-

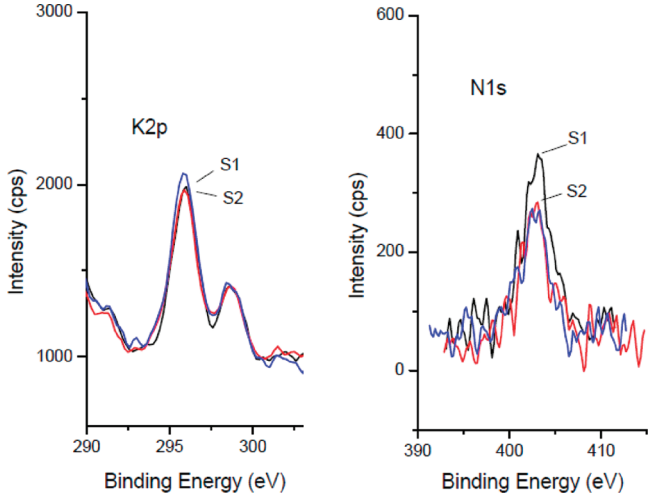

FIGURE 3. XPS spectra in the K(2p) and N(1s) regions. The spectra for S1-DNA (S1) and S2-DNA (S2) are indicated. The potassium and nitrogen signals are due to the potassium component in glass substrate and deposited silanized DNA, respectively.

lanized DNA. The deposition procedure and conditions are closely related to the one concerning the microarray probes. In Figure 3, we present the binding-energy regions for potassium component contained in glass and for nitrogen due to DNA bases. The potassium region for the three silane-DNA systems reveals closely similar intensities, indicating similar thickness of the silane-DNA adlayers. Importantly, considering the N1s spectra in Figure 3, the higher fluorescence intensity upon the hybridization reaction for the immobilized S2-DNA probes, as compared with the S1 and S3 systems, cannot be explained with a correspondingly higher DNA surface density. In fact, the S1-DNA N1s intensity is somewhat higher than in the case of the S2-DNA system. Therefore, the XPS data point to a silane cause of the observed fluorescence intensity variations.

This influence of the silane functionally is in agreement with other type of studies. Generally, the chemistry of the reactive organosilicon compounds R_nSiX_{3-n}, (X = methoxy or ethoxy) is complex. It involves a number of steps, whereby, in the presence of water, initially hydrolysis of the alkoxy groups occurs. It is after the first and second alkoxy groups are hydrolyzed that condensation to siloxane oligomers follows. On the other hand, it has been shown that the condensation reaction at a surface depends sensitively on the structure of silane. Thus, in a study (16) of the reaction of silica with various aminopropyl-alkoxysilanes probed by fluorescein (FITC) labeling, the uniformity of the amine site distribution on the silica surface is found to be mainly determined by the number of alkoxy groups. Monoalkoxysilanes are generally distributed more uniformly than trialkoxysilanes and the fluorescence intensity of the FITC-coupled samples is maximized by reducing the functionality of the silanes acting as surface anchors. The differences between the ethoxy groups and methoxy groups, on the other hand, had a negligible effect on the aminosilane surface densities (16) despite the fact that ethoxysilanes are more bulky than the corresponding methoxysilanes. In a different study (17), self-assembled 3-mercaptopropyltri-

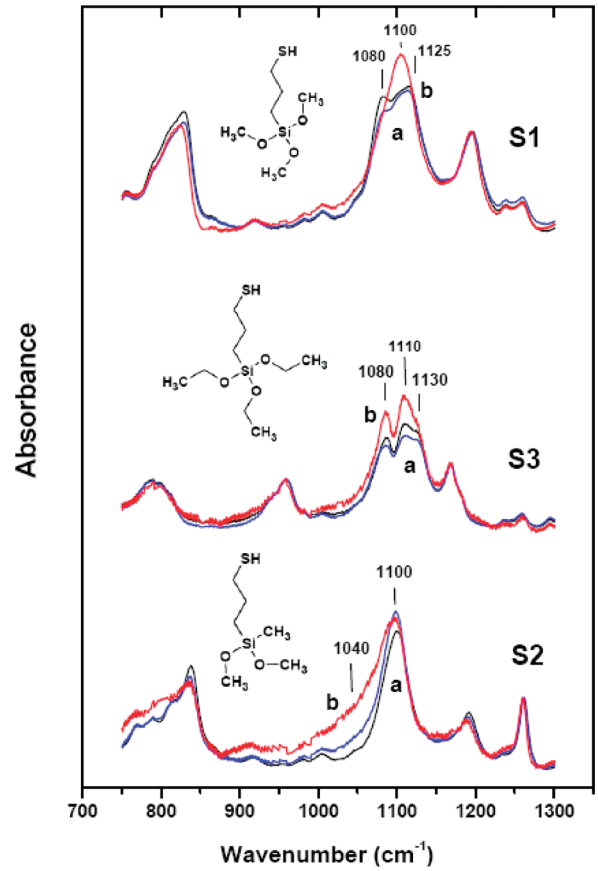

FIGURE 4. Normalized reflection−absorption FTIR spectra of thin films of silanes deposited on gold surface by spin-coating (10 mM silanes in NaOAc buffer, pH 4.3). The three different spectra for each silane show the time dependence during continuous monitoring of the infrared signatures: After the initial spectrum (a), the follow-up spectra were taken 15 and 60 min (spectrum b) later.

methoxysilane (S1) layers on hydroxyl-terminated silicon oxide were characterized with various techniques and found to form dispersed islands of 20−200 nm in diameter. The nonuniform distribution and density manifest itself in low fluorescence intensities after the FITC coupling (17). Therefore, the degree and nature of silane clustering (condensation) seems to be determined mainly by the number rather than the chemical nature of the alkoxy groups. Because of the reduced functionality, the structural complexity of the interfacial layer composed of difunctional silane S2 should be less than those of the trifunctional silanes.

However, structural information is scarce for difunctional organosilanes (R_2SiX_2), the least studied reactive silanes. For this reason we have compared the condensation behavior of the spin-coated silane films by means of time dependent FTIR spectra (Figure 4). It is known that in spin-cast films the mole fraction of the retained solvent increases as the film thickness decreases into the nanometer range (18). We estimate from the literature (19) that the film thickness in this study should be in the range of 30−100 nm, implying that the deposited films contain sufficient water for the hydrolyses of the alkoxy group and the following condensation reaction. In the spectra in Figure 4, the bands due to asymmetric Si−O−Si stretching vibration are found in the region 1040−1130 cm^{-1}. The band pattern may be used to

distinguish between cyclic and linear polysiloxanes (20). Long chain siloxanes have two broad bands in the region 1000−1100 cm^{-1}. Because of the influence of ring chain, cyclic siloxane trimers absorb at 1010−1020 cm^{-1}, which is about 60 cm^{-1} less than other cyclic siloxanes, whereas tetramers (which have less ring strain) absorb at 1070−1090 cm^{-1} along with high cyclic siloxanes. Linear small-chain siloxanes tend to absorb at about 1050 cm^{-1} and with increase in the molecular weight, this band gradually broadens to occupy the region 1000−1100 cm^{-1}. As evident in Figure 4, the spectra of trifunctional silanes S1 and S3 reveal intense bands at 1080 cm^{-1}, 1100 cm^{-1} and 1130 cm^{-1} which increase in intensity with time and are characteristic of cyclic siloxanes. Such structures would enforce unfavorable conformations of attached DNA. In contrast, the difunctional silane S2 shows an increase in the intensity only around 1040 cm^{-1}, indicating the formation of short linear siloxane chains. This type of short structures allow for a strong bonding to the surfaces, reinforced through the two-dimensional Si−O−Si condensation, and at the same time permit a DNA conformation extending farther away from the surface, this being favorable for its reaction with the complementary strand.

In conclusion, our fluorescence and FTIR data clearly indicate that the use of difunctional alkoxysilanes instead widely used trifunctional silanes to silanize and immobilize DNA on glass is more favorable for the DNA microarray applications. The decisive role of silane revealed in this work makes it likely that further significant improvements are possibly by adroit choice of the silane DNA tethers.

Acknowledgment. We Deutsche Forschungsgesellschaft (DFG) for the financial support, and Dr. C. Hultschig of the Max-Planck Institute for Molecular Genetics (Molgen) Berlin for the printing of the microarrays.

REFERENCES AND NOTES

(1) Schena, M.; Shalon, D.; Davis, R. W.; Brown, P. O. *Science* **1995**, *270*, 467–470.
(2) Liu, Q.; Wang, L.; Frutos, A. G.; Condon, A. E.; Corn, R. M.; Smith, L. M. *Nature* **2000**, *403*, 175–179.
(3) Bashir, R. *Superlattices Microstruct.* **2001**, *29*, 1–16.
(4) Palchetti, I.; Mascini, M. *Top. Curr. Chem.* **2006**, *261*, 27–43.
(5) Hansma, H. G.; Revenko, I.; Kim, K.; Laney, D. E. *Nucl. Acids Res.* **1996**, *24*, 713–720.
(6) Klein, D. C. G.; Janssen, J. W.; Kouwenhoven, L. P. *Appl. Phys. Lett.* **2001**, *78*, 2396–2398.
(7) Kaufmann, R.; Averbukh, I.; Naaman, R. *Langmuir* **2008**, *24*, 927–931.
(8) Steel, A. B.; Levicky, R. L.; Herne, T. M.; Tarlov, M. J. *Biophys. J.* **2000**, *79*, 975–981.
(9) Beier, M.; Hoheisel, J. D. *Nucl. Acids Res.* **1999**, *27*, 1970–1977.
(10) Rogers, Y. H.; Jiang-Baucom, P.; Huang, Z. J.; Bogdanov, V.; Anderson, S.; Boyce-Jacino, M. T. *Anal. Biochem.* **1999**, *266*, 23–30.
(11) Lipshutz, R. J.; Fodor, S. P.; Gingeras, T. R.; Lockhart, D. J. *Nat. Genet.* **1999**, *21*, 20–24, and references therein.
(12) Möller, R.; Csaki, A.; Köhler, J. M.; Fritzsche, W. *Nucl. Acid. Res.* **2000**, *28*, e91.
(13) Kumar, A.; Larsson, O.; Parodi, D.; Liang, Z. *Nucl. Acid. Res.* **2000**, *28*, e71.
(14) Kasry, A.; Borri, P.; Davies, P. R.; Harwood, A.; Thomas, N.; Lofas, S.; Dale, T. *ACS Appl. Mater. Interfaces* **2009**, *1*, 1793–1798.
(15) Britt, D. W.; Hlady, V. *Langmuir* **1999**, *15*, 1770–1776.
(16) Salmio, H.; Bruhwiler, D. *J. Phys. Chem. C* **2007**, *111*, 923–929.
(17) Hu, M.; Noda, S.; Okubo, T.; Yamaguchi, Y.; Komiyama, H. *Appl. Surf. Sci.* **2001**, *181*, 307–316.
(18) Garcia-Turiel, J.; Jerome, B. *Colloid Polym. Sci.* **2007**, *285*, 1617–1623.
(19) Extrand, C. W. *Langmuir* **1993**, *9*, 475–480.
(20) Wachholz, S.; Keidel, F.; Just, U.; Geissler, H.; Käppler, K. *J. Chromatgr., A* **1995**, *693*, 89–99.

AM100263T